Int. J. Solids Structures, 1977, Vol. 13, pp. 897–912. Pergamon Press. Printed in Great Britain

LINEAR AND NONLINEAR ANALYSIS OF STIFFENED PLATES

R. S. SRINIVASAN
Department of Applied Mechanics, Indian Institute of Technology, Madras 600 036, India

and

S. V. RAMACHANDRAN
Department of Civil Engineering, Regional Engineering College, Calicut 673 601, India

(*Received 5 January* 1977)

Abstract—An analysis is presented for the large deflection of clamped laterally loaded skew plates with stiffeners parallel to the skew directions. The governing nonlinear differential equations are derived taking into account the eccentricity of the stiffeners. A numerical procedure involving the use of integral equations of beams and the Newton–Raphson method is employed to get the solution. Numerical work has been done. The effect of variation of skew angle and size of stiffener on the behaviour of the stiffened skew plate has been studied.

NOTATIONS

A_α, A_β area of stiffeners in the directions α and β
B_α, B_β breadth of stiffeners in the directions α and β
D_α, D_β depth of stiffeners in the directions α and β
D, $\bar{D}$: $Eh^3/\{12(1-\nu^2)\}$, $E\bar{h}^3/\{12(1-\nu^2)\}$ flexural rigidities
E Young's modulus
E_α, E_β Young's moduli of stiffeners in the direction α and β
I_α, I_β second moment of the stiffeners about the middle plane of the plate
$M_\alpha, M_\beta, M_{\alpha\beta}$; $N_\alpha, N_\beta, N_{\alpha\beta}$ bending moments and membrane forces
Q, $\bar{Q}$: $qb^4/(Dh)$, $qb^4/(\bar{D}\bar{h})$ non-dimensional intensity of lateral load
R b/a = aspect ratio
S_B, S_T: $\sigma_B(1-\nu^2)/(E\bar{h}^2)$, $\sigma_T(1-\nu^2)/(E\bar{h})$ non-dimensional stresses at points B and T
S_α, S_β first moment of the stiffeners about the middle plane of the plate
U, V: ua/h^2, va/h^2 non-dimensional inplane displacements
W, $\bar{W}$: w/h, $w/\bar{h}$ non-dimensional lateral displacement
a, b sides of the plate
b_α, b_β spacing of stiffeners in the directions α and β
$h, \bar{h}$ thickness of plate
q intensity of lateral load
r_{PT} ratio of volume of deck plate to total volume of deck plate and stiffeners
u, v displacements of the middle plane of the plate in the directions α and β
w displacements of the middle plane of the plate in the lateral, i.e. z direction
x, y, z orthogonal co-ordinates
α, β oblique co-ordinates
$\epsilon_x, \epsilon_y, \gamma_{xy}$ strains of the middle surface of the plate in the orthogonal directions x and y
$\epsilon_\alpha, \epsilon_\beta, \gamma_{\alpha\beta}$ strains of the middle surface of the plate in the oblique directions α and β
θ included angle
$\sigma_x, \sigma_y, \tau_{xy}$ stresses with reference to the co-ordinates x and y
$\sigma_\alpha, \sigma_\beta, \tau_{\alpha\beta}$ stresses with reference to the co-ordinates α and β
σ_B, σ_T stresses at points B and T
θ skew angle
ν Poisson's ratio
ξ, η: α/a, β/b non-dimensional oblique co-ordinates.

INTRODUCTION

Stiffened plates are extensively used in different types of structures. If the stiffeners are closely spaced, the effect of the stiffeners can be "smeared out" over the area of the plate and an analysis can be done by considering an equivalent plate of uniform thickness.

When the stiffners are orthogonal, the equivalent plate can be treated as orthotropic plate. But there are situations, where the stiffeners are not provided orthogonally. For example, in the case of a skew plate, stiffeners may be provided along the skew directions. In this case, the equivalent plate has to be considered as anisotropic. If the stiffeners are eccentric (with respect to the plate), the middle surface of the plate will be subjected to inplane stresses even when the deflections are small. Therefore the eccentricity of stiffeners must be properly taken into account.

Au *et al.*[1] have presented an analysis for a laterally loaded rectangular plate with eccentric stiffeners in orthogonal directions. Mcelman *et al.*[2] have provided a theoretical analysis for the buckling and free vibration of eccentricalty stiffened cylindrical shells and flat plates. Soper[3] has analysed orthogonally stiffened rectangular plates in the large deflections range when subjected to lateral load. All the above authors have considered an equivalent orthotropic plate for their analyses by smearing the effect of the stiffeners and they have used trigonometric series for their solutions. To the authors' knowledge there is no literature for the linear and nonlinear analysis of clamped stiffened skew plate.

Hence in this paper, the large deflection analysis of laterally loaded skew plate with eccentric stiffeners parallel to the skew directions is considered. The governing nonlinear differential equations are derived taking into account the eccentricity of stiffeners and a numerical solution is obtained making use of the integral equation method[4, 5].

DERIVATION OF EQUATIONS

The oblique and rectangular co-ordinate axes and the plan of the skew plate with stiffeners are shown in Fig. 1. It is to be noted that the spacing of the stiffeners is measured in a direction perpendicular to the stiffeners.

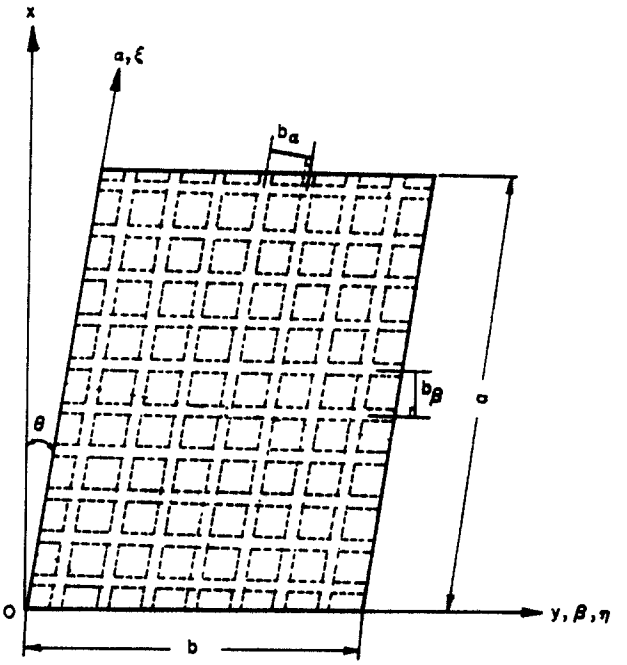

Fig. 1. Sketch showing the systems of co-ordinate axes and the plan of skew plate with stiffners.

Definition of oblique stresses

In order to include the stresses in the stiffeners in calculating the stress resultants (to be used in the subsequent derivations), the oblique system of stresses is defined following Argyris[6]. Referring to Fig. 2, the normal stress σ_α is defined as the force per unit area along *de* (i.e.) perpendicular to the α direction. Similarly $\tau_{\alpha\beta}$ is the shear force per unit area along *de* but acting along *dc*. In a similar manner σ_β and $\tau_{\alpha\beta}$ can be defined with respect to *df*. It may be noted that the "true stresses" are those given by the orthogonal system shown in Fig. 3,

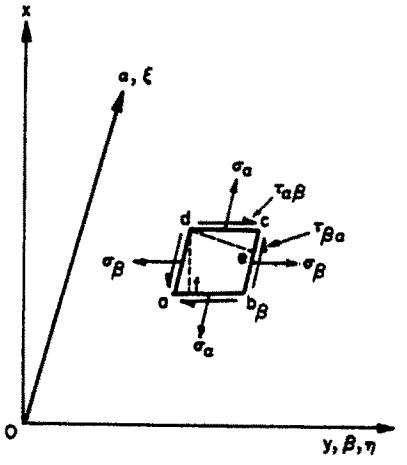

Fig. 2. Oblique system of stresses.

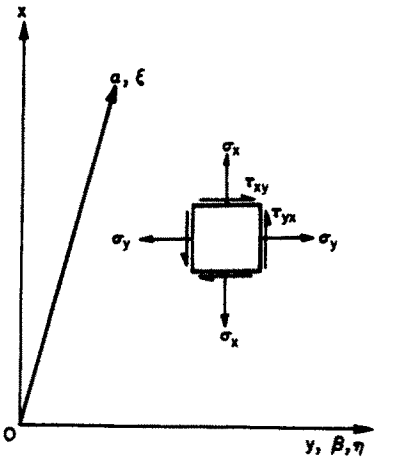

Fig. 3. Orthognal system of stresses.

whereas the oblique stresses defined are but "psuedo stresses" introduced for the purpose of convenience in making the derivations.

Relations between the oblique and orthogonal system of stresses

In Fig. 4(a), the wedge OAB is acted upon by stresses in the oblique directions and in Fig. 4(b), the corresponding stresses in rectangular directions are shown. Equating the forces acting on the faces AB and OB, the following relations can be obtained.

$$\begin{Bmatrix} \sigma_\alpha \\ \sigma_\beta \\ \tau_{\alpha\beta} \end{Bmatrix} = \begin{bmatrix} \sec^2\theta & 0 & 0 \\ \tan^2\theta & 1 & -2\tan\theta \\ -\sec\theta\tan\theta & 0 & \sec\theta \end{bmatrix} \begin{Bmatrix} \sigma_x \\ \sigma_y \\ \tau_{xy} \end{Bmatrix}$$

i.e.

$$\{\sigma_0\} = [A]\{\sigma_R\} \tag{1}$$

where the subscripts 0 and R refer to oblique and rectangular co-ordinate systems respectively.

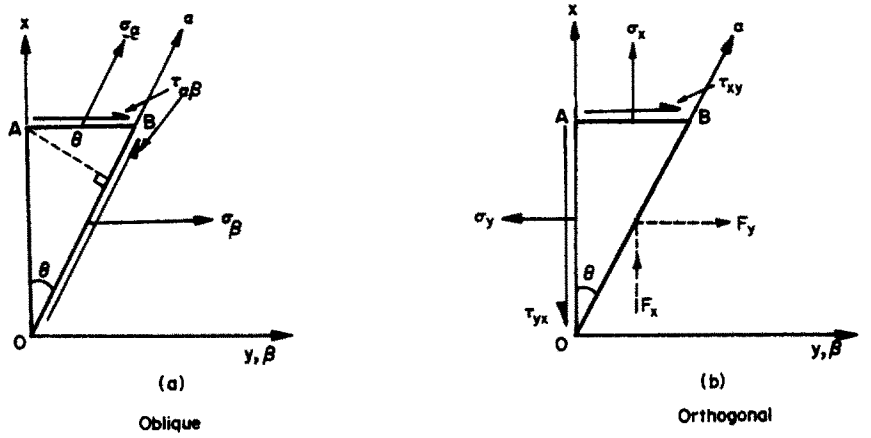

Fig. 4. Stresses in a wedge.

Relations between the strains in the two systems

The relations between the strains in the rectangular and oblique co-ordinate systems can be stated as follows (vide Morley[7])

$$\begin{Bmatrix} \epsilon_x \\ \epsilon_y \\ \gamma_{xy} \end{Bmatrix} = \begin{bmatrix} \sec^2\theta & \tan^2\theta & -\tan\theta\sec\theta \\ 0 & 1 & 0 \\ 0 & -2\tan\theta & \sec\theta \end{bmatrix} \begin{Bmatrix} \epsilon_\alpha \\ \epsilon_\beta \\ \gamma_{\alpha\beta} \end{Bmatrix}$$

i.e.

$$\{\epsilon_R\} = [C]\{\epsilon_0\}. \tag{2}$$

Stress-strain relations in rectangular co-ordinates

For an isotropic material the stress-strain relations in the rectangular co-ordinates can be written as follows.

$$\begin{Bmatrix} \sigma_x \\ \sigma_y \\ \tau_{xy} \end{Bmatrix} = \frac{E}{(1-\nu^2)} \begin{bmatrix} 1 & \nu & 0 \\ \nu & 1 & 0 \\ 0 & 0 & (1-\nu)/2 \end{bmatrix} \begin{Bmatrix} \epsilon_x \\ \epsilon_y \\ \gamma_{xy} \end{Bmatrix}$$

i.e.

$$\{\sigma_R\} = [B]\{\epsilon_R\}. \tag{3}$$

Stress-strain relations in the oblique system

Making use of eqns (1)–(3),

$$\{\sigma_0\} = [A]\{\sigma_R\} = [A][B]\{\epsilon_R\} = [A][B][C]\{\epsilon_0\} = [D]\{\epsilon_0\} \quad \text{(say)} \tag{4}$$

i.e.

$$\begin{Bmatrix} \sigma_\alpha \\ \sigma_\beta \\ \tau_{\alpha\beta} \end{Bmatrix} = \frac{E}{(1-\nu^2)} \begin{bmatrix} d_{11} & d_{12} & d_{13} \\ d_{21} & d_{22} & d_{23} \\ d_{31} & d_{32} & d_{33} \end{bmatrix} \begin{Bmatrix} \epsilon_\alpha \\ \epsilon_\beta \\ \gamma_{\alpha\beta} \end{Bmatrix} \tag{5}$$

in which

$$d_{11} = \sec^4\theta; \qquad d_{12} = \sec^2\theta(\nu + \cot^2\theta)$$

$$d_{13} = -\tan\theta\sec^3\theta; \qquad d_{21} = d_{12}$$

$$d_{22} = d_{11}; \qquad d_{23} = d_{13}$$

$$d_{31} = d_{13}; \qquad d_{32} = d_{23}$$

and

$$d_{33} = \tan^2\theta\sec^2\theta + \{(1-\nu)/2\}\sec^2\theta.$$

Strain-displacement relations

When the lateral deflections are large compared to the thickness of the plate, the strain displacement relations are

$$\epsilon_\alpha = u_{,\alpha} + (w_{,\alpha})^2/2$$

$$\epsilon_\beta = v_{,\beta} + (w_{,\beta})^2/2 \tag{6a–c}$$

$$\gamma_{\alpha\beta} = u_{,\beta} + v_{,\alpha} + w_{,\alpha}w_{,\beta}.$$

Following Kirchoff's assumptions the strains at any point with distance z from the middle surface of the plate can be written as

$$\epsilon_\alpha(z) = \epsilon_\alpha - zw_{,\alpha\alpha}$$

$$\epsilon_\beta(z) = \epsilon_\beta - zw_{,\beta\beta} \tag{7a–c}$$

$$\gamma_{\alpha\beta}(z) = \gamma_{\alpha\beta} - 2zw_{,\alpha\beta}.$$

Expressions for stress resultants

With the help of the relations derived earlier, it is now possible to express the stress resultants in terms of the displacements of the middle surface of the plate as follows.

$$
\begin{aligned}
N_\alpha &= \int_{-h/2}^{h/2} \sigma_\alpha \, dz + \frac{1}{b_\alpha} \int_S E_\alpha \epsilon_\alpha(z) \, dA \\
N_\beta &= \int_{-h/2}^{h/2} \sigma_\beta \, dz + \frac{1}{b_\beta} \int_S E_\beta \epsilon_\beta(z) \, dA \\
N_{\alpha\beta} &= N_{\beta\alpha} = \int_{-h/2}^{h/2} \tau_{\alpha\beta} \, dz \\
M_\alpha &= \int_{-h/2}^{h/2} \sigma_\alpha z \, dz + \frac{1}{b_\alpha} \int_S E_\alpha \epsilon_\alpha(z) z \, dA \\
M_\beta &= \int_{-h/2}^{h/2} \sigma_\beta z \, dz + \frac{1}{b_\beta} E_\beta \epsilon_\beta(z) z \, dA \\
M_{\alpha\beta} &= M_{\beta\alpha} = \int_{-h/2}^{h/2} \tau_{\alpha\beta} z \, dz,
\end{aligned}
\tag{8a–f}
$$

where S indicates that the integration is to be performed over the cross sectional area of the stiffener.

In the case of $N_{\alpha\beta}$, the horizontal shear stresses in the stiffener have been neglected in comparison with those in the plate. Similarly, in determining $M_{\alpha\beta}$, the contribution from the stiffener has been ignored since the stiffeners are considered to be slender and open-web type.

Equations of equilibrium

Considering an element of the plate, the equations of equilibrium of forces in the α, β and z directions can be written as follows:

$$
\begin{aligned}
N_{\alpha,\alpha} + N_{\alpha\beta,\beta} &= 0 \\
N_{\beta,\beta} + N_{\alpha\beta,\alpha} &= 0 \\
M_{\alpha,\alpha\alpha} + 2M_{\alpha\beta,\alpha\beta} + M_{\beta,\beta\beta} &= -q - [N_\alpha w_{,\alpha\alpha} + 2N_{\alpha\beta} w_{,\alpha\beta} + N_\beta w_{,\beta\beta}].
\end{aligned}
\tag{9a–c}
$$

Substituting eqns (8a–f) in eqns (9a–c) and using the non-dimensional quantities given under notations, the equations of equilibrium can be expressed as follows.

$$
\begin{aligned}
&a_1 U_{,\xi\xi} + a_2 U_{,\xi\eta} + a_3 U_{,\eta\eta} + a_4 V_{,\xi\xi} + a_5 V_{,\xi\eta} + a_6 V_{,\eta\eta} + a_7 W_{,\xi\xi\xi} \\
&\quad = [a_{11} W_{,\xi\xi} + a_{21} W_{,\xi\eta} + a_{31} W_{,\eta\eta}] W_{,\xi} + [a_{12} W_{,\xi\xi} + a_{22} W_{,\xi\eta} + a_{32} W_{,\eta\eta}] W_{,\eta}
\end{aligned}
\tag{10a}
$$

$$
\begin{aligned}
&b_1 U_{,\xi\xi} + b_2 U_{,\xi\eta} + b_3 U_{,\eta\eta} + b_4 V_{,\xi\xi} + b_5 V_{,\xi\eta} + b_6 V_{,\eta\eta} + b_7 W_{,\eta\eta\eta} \\
&\quad = [b_{11} W_{,\xi\xi} + b_{21} W_{,\xi\eta} + b_{31} W_{,\eta\eta}] W_{,\xi} + [b_{12} W_{,\xi\xi} + b_{22} W_{,\xi\eta} + b_{32} W_{,\eta\eta}] W_{,\eta}
\end{aligned}
\tag{10b}
$$

$$
\begin{aligned}
&c_1 W_{,\xi\xi\xi\xi} + c_2 W_{,\xi\xi\xi\eta} + c_3 W_{,\xi\xi\eta\eta} + c_4 W_{,\xi\eta\eta\eta} + c_5 W_{,\eta\eta\eta\eta} + c_6 U_{,\xi\xi\xi} + c_7 V_{,\eta\eta\eta} \\
&\quad = Q + [c_{11} U_{,\xi} + c_{12} U_{,\eta} + c_{13} V_{,\xi} + c_{14} V_{,\eta} + c_{15}(W_{,\xi})^2 + c_{16}(W_{,\xi})(W_{,\eta}) + c_{17}(W_{,\eta})^2] W_{,\xi\xi} \\
&\qquad + [c_{21} U_{,\xi} + c_{22} U_{,\eta} + c_{23} V_{,\xi} + c_{24} V_{,\eta} + c_{25}(W_{,\xi})^2 + c_{26}(W_{,\xi})(W_{,\eta}) + c_{27}(W_{,\eta})^2] W_{,\xi\eta} \\
&\qquad + [c_{31} U_{,\xi} + c_{32} U_{,\eta} + c_{33} V_{,\xi} + c_{34} V_{,\eta} + c_{35}(W_{,\xi})^2 + c_{36}(W_{,\xi}) + c_{37}(W_{,\eta})^2] W_{,\eta\eta}.
\end{aligned}
\tag{10c}
$$

The coefficients a_1, b_1, c_1 etc. are given in Appendix A.

Boundary conditions

The plate is assumed to be clamped and rigidly held in position along the edges. This boundary condition may be stated as:

$$\text{(a)} \quad \text{along } \xi = 0, 1; \qquad W = W_{,\xi} = U = V = 0$$
$$\text{(b)} \quad \text{along } \eta = 0, 1; \qquad W = W_{,\eta} = U = V = 0. \tag{11a, b}$$

Method of solution

Considering discrete points along lines parallel to the skew co-ordinates, a numerical solution to the differential equations satisfying the boundary conditions can be obtained by the integral equations method [4, 5].

Let the highest derivatives of W be denoted by

$$W_{,\xi\xi\xi\xi} = k(\xi, \eta); \qquad W_{,\eta\eta\eta\eta} = l(\xi, \eta). \tag{12a, b}$$

For points along the line $\eta = \eta_\eta$ (Fig. 1), eqn (12a) can be represented as

$$W(\xi, \eta_\eta) = \int_0^1 g(\xi, \psi; \eta_\eta) k(\psi; \eta_\eta)\, d\psi \tag{13}$$

where $g(\xi, \psi; \eta_\eta)$ is the Green's function of the boundary value problem $W_{,\xi\xi\xi\xi} = 0$ with the boundary conditions $W = W_{,\xi} = 0$ at $\xi = 0, 1$.

The integration indicated in eqn (13) can be performed as summation using Simpson's rule and the above equation can be represented in matrix form. Considering various lines parallel to ξ axis, they can be combined and written as

$$\{W\} = [A]\{k\}. \tag{14}$$

Similarly considering lines parallel to η axis, eqn (12b) can be expressed as

$$\{W^*\} = [B]\{l^*\} \tag{15}$$

where * indicates that the discrete points are reckoned along lines parallel to η axis. Making use of a unitary transformation matrix $[T]$ such that

$$\{W^*\} = [T]\{W\}; \qquad \{l^*\} = [T]\{l\} \tag{16a, b}$$

$$\{W\} = [T]^{-1}\{W^*\} = [T]^{-1}[B]\{l^*\} = [T]^{-1}[\bar{B}][T]\{l\} = [\bar{B}]\{l\}. \tag{17}$$

Using derivatives of Green's functions one gets

$$\{W_{,\xi}\} = [A_{,\xi}]\{k\} = [A_{,\xi}][A^{-1}]\{W\}$$
$$\{W_{,\eta}\} = [\bar{B}_{,\eta}]\{l\} = [\bar{B}_{,\eta}][\bar{B}^{-1}]\{W\} \tag{18a, b}$$

giving

$$\frac{\partial}{\partial \xi} = [A_{,\xi}][A^{-1}] \qquad \text{and} \qquad \frac{\partial}{\partial \eta} = [\bar{B}_{,\eta}][\bar{B}^{-1}].$$

Now any derivative of W can be expressed in terms of the single unknown $\{l\}$.

For example,

$$\{W_{,\xi\xi\eta\eta}\} = [A_{,\xi\xi}][A^{-1}][\bar{B}_{,\eta\eta}]\{l\}$$
$$\{W_{,\xi\eta}\} = [A_{,\xi}][A^{-1}][\bar{B}_{,\eta}]\{l\}$$
$$\{W_{,\eta\eta}\} = [\bar{B}_{,\eta\eta}]\{l\}.$$

An inspection of eqns (10a–c) reveals that the order of the highest derivative of U and V is three and these terms result as a consequence of the eccentricity of the stiffeners. In general, for boundary value problems, the order of the highest derivative is even, say $2n$, such that n

boundary conditions can be specified at either end. Therefore, in this case the third derivative cannot be taken as the unknown. Instead, the second derivative is considered as the unknown and the relevant boundary conditions are satisfied. The values of the third derivative at the grid points are obtained from the values of the second derivatives. This is done by fitting a suitable curve and finding its gradient at the grid points. In this investigation a 4th degree curve is fitted considering five grid points at a time and the derivatives are found therefrom. Thus

$$\{U_{,\xi\xi\xi}\} = [D_d]\{U_{,\xi\xi}\}$$
$$\text{and} \qquad \{V_{,\eta\eta\eta}\} = [\tilde{D}_d]\{V_{,\eta\eta}\} \qquad (19a, b)$$

where $[D_d]$ is the matrix to obtain third derivatives from second derivatives, $[\tilde{D}_d] = [T]^{-1}[D][T]$ and $[T]$ = unitary transformation matrix.

Assuming

$$U_{,\eta\eta} = s(\xi, \eta); \qquad V_{,\eta\eta} = n(\xi, \eta), \qquad (20a, b)$$

making use of Green's functions appropriate to the boundary conditions in question and following a procedure similar to the one adopted for W, it is possible to express any derivative of U and V in terms of s and n respectively.

The differential eqns (10a–c) can now be converted into algebraic equations in matrix form as follows:

$$[A_1]\{s\} + [A_2]\{n\} = \{R_1\}$$
$$[B_1]\{s\} + [B_2]\{n\} = \{R_2\} \qquad (21a–c)$$
$$[C_1]\{l\} = \{Q\} + \{R_3\} * \{R_4\} + \{R_5\} * \{R_6\} + \{R_7\} * \{R_8\} + \{R_9\} + \{R_{10}\}$$

where

$$\{R_1\} = [M_1]\{l\}; \qquad \{R_2\} = [M_2]\{l\}; \ \ldots \ \{R_8\} = [M_8]\{l\}$$
$$\{R_9\} = [M_9]\{s\}; \qquad \{R_{10}\} = [M_{10}]\{n\}$$
$$\{Q\} = \text{the load vector.}$$

The * multiplication in the above equation is defined as follows.

$$\{C\} = \{A\} * \{B\}$$

means

$$C_i = a_i b_i \qquad \text{(no sum on the index } i\text{)}.$$

The matrices A_1, B_1, C_1, M, etc. are appropriate rectangular matrices.

A solution to this set of nonlinear algebraic equations is obtained by using the Newton–Raphson procedure [5, 8].

RESULTS AND DISCUSSIONS

Numerical results have been obtained for a limited data in order to show the workability of the formulation and computer program. In preparing the computer programs, advantage has been taken of the skew symmetry and skew anti-symmetry of the vectors $\{l\}$, $\{s\}$ and $\{n\}$ in order to reduce the size of the matrices and save computer time.

At any value of the load, the Newton–Raphson iterations are continued till the results converge. For this purpose, the deflection at centre is used as the criterion. If the values of central deflection in two consecutive iterations do not differ by more than 0.01% of their value, then the iterations are terminated. The gradient calculated for any load is used for a few more load increments until its accuracy becomes poor as indicated by the increase in the number of iterations required for convergence. The gradient is updated when the number of iterations exceed 10.

Considering an element of the skew plate with stiffeners (Fig. 1),

$$\frac{\text{(volume of deck plate per unit area)}}{\text{(total volume of plate and stiffeners per unit area)}} = \frac{h}{\bar{h}} = r_{PT}$$

where $\bar{h} = h + (A_\alpha/b_\alpha) + (A_\beta/b_\beta)$.

It may be verified that if $r_{PT} = 1$, it represents a plate without stiffeners. A value of $r_{PT} < 1$ indicates that part of the material from plate is removed and placed as stiffeners. However the total volume per unit area remains the same for all values of r_{PT}. Thus by varying r_{PT}, it is possible to get plates with different allocations of volumes between deck plate and stiffeners. In this paper it is proposed to study the change in the behaviour of the plate by varying r_{PT} and this can be done by changing the dimensions of the stiffeners (viz) width, depth and spacing. In order to limit the number of variables, the spacing and depth of stiffeners are taken as constant multiples of the thickness of the deck plate and width of the stiffener respectively.

Let the width, depth and spacing of stiffeners in "α" direction be $B_{\alpha h}h$, $D_{\alpha h}h$ and $b_{\alpha h}h$ respectively.

Assuming that identical stiffeners are provided along both the skew directions,

$$r_{PT} = \frac{1}{1 + 2[B_{\alpha h}^2 r_{DB}/b_{\alpha h}]}$$

where $r_{DB} = D_\alpha h/B_{\alpha h}$.

Therefore the width of the stiffener corresponding to a given value of r_{PT} can be determined as

$$B_{\alpha h} = [(1/r_{PT}) - 1][b_{\alpha h}/(2r_{DB})].$$

From the governing eqns (10a–c) it can be inferred that the solution for displacements and stresses will be obtained in terms of h, the thickness of the deck plate. However it will be convenient for purposes of comparison, if these quantities are expressed in terms of a constant thickness. For this purpose, $\bar{h}$, the thickness of the equivalent plate of uniform thickness having the same volume is taken as the reference.

For each case, in addition to the deflection at centre, the normal stresses (in the direction of stiffeners) at the centre of the plate corresponding to B, the bottom of the stiffener and T, the top of the deck plate (see Fig. 6 and 7) have also been calculated.

Convergence study

For a plate with $\theta = 45°$, $R = 1$ and $r_{PT} = 0.67$, the results of a convergence study are presented in Table 1, for three values of the load parameter $\bar{Q}$, which cover both linear and nonlinear ranges. For all the three loads, the convergence can be seen to be good.

Table 1. Conovergence study, $\theta = 45°$; $R = 1$; $\nu = 0.3$; $r_{PT} = 0.67$.

Mesh		$\bar{Q} = 252.9$			$\bar{Q} = 5563.6$			$\bar{Q} = 16943.6$		
M	N	$\bar{W}$	S_B	S_T	$\bar{W}$	S_B	S_T	$\bar{W}$	S_B	S_T
1/4	9	0.0589	2.221	−0.787	1.005	41.67	−10.82	1.843	77.87	−11.83
1/6	25	0.0596	2.222	−0.805	1.039	38.43	−10.00	1.969	70.50	−9.38
1/8	49	0.0595	2.218	−0.802	1.034	38.33	−9.71	2.000	69.93	−9.13

Note: Mesh size = M × side; N = Number of interior mesh points.

Small deflections

The linearised form of eqns (10a–c) will correspond to the case of small deflections theory and a solution to the vectors $\{l\}$, $\{s\}$ and $\{n\}$ can be obtained by solving these simultaneous equations.

For the value of $R = 1$, deflection and stresses at centre have been obtained for plates with $\theta = 0°$, 30° and 45° for different values of the ratio r_{PT}. These results are shown in Figs. 5–7. The

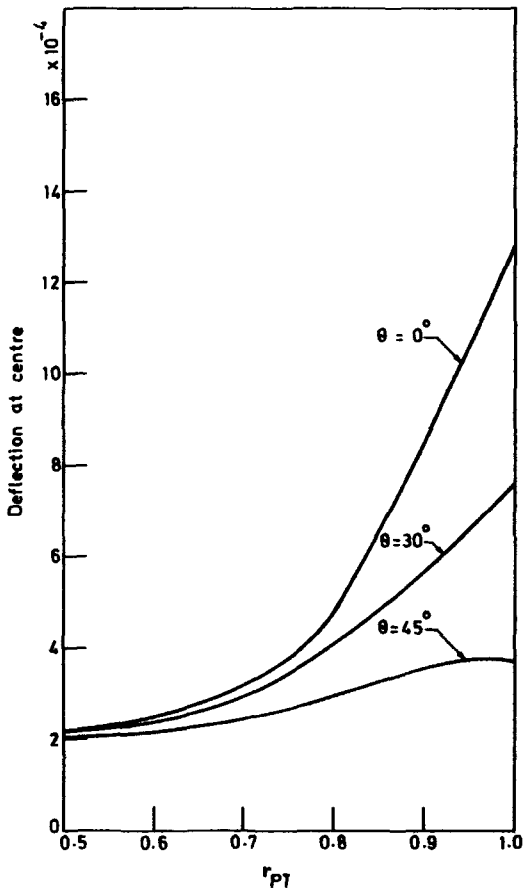

Fig. 5. r_{PT} vs deflection at centre.

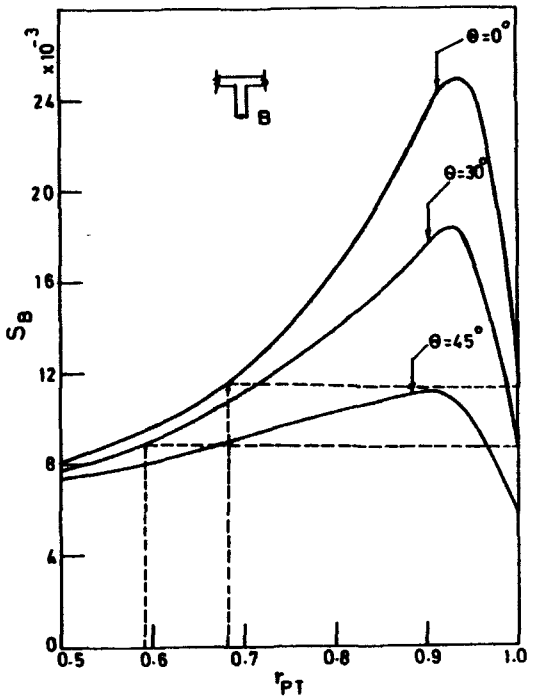

Fig. 6. r_{PT} vs stress at point B.

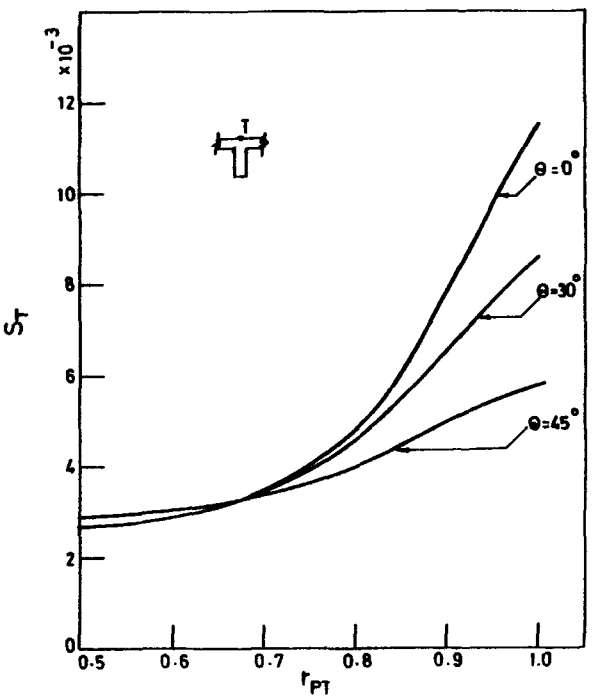

Fig. 7. r_{PT} vs stress at point T.

values of r_{DB} and b_{ah} have been taken as 4 and 16 respectively and $E_\alpha = E_\beta = E$ of the plate.

As the value of r_{PT} is decreased from 1.0, i.e. by putting more and more material in the stiffeners, the deflection reduces considerably, the reduction being the maximum for $\theta = 0°$.

In Fig. 6, initially there is an increase in the stress at B, as r_{PT} is decreased from 1.0 to about 0.9. Thereafter the stress decreases with decrease in r_{PT}. In the case of $\theta = 45°$, for all values of $r_{PT} < 1$, the stress at B is found to be higher than the corresponding value for the plate without stiffeners, i.e. for $r_{PT} = 1$. However, for $\theta = 0°$ (and 30°), a value of $r_{PT} < 0.68$ (0.58) represents a plate for which both deflection and stress at centre are less than the corresponding values for a plate without stiffeners but having the same volume.

At $r_{PT} = 0.5$, there is no appreciable difference in the deflection for the different values of the skew angle. This is also true with regard to the stresses. This might be due to the fact, that for this value of r_{PT}, the structure behaves more like a grid.

Large deflections

Figures 8–10 show the graphs of Load vs Deflection at centre, Figs. 11–13 the graphs of Load vs Stress at B and Figs. 14–16 the graphs of Load vs Stress at T. With reference to these figures the following observations can be made.

(1) When the load is small (see Fig. 8), for any value of the load, the deflection decreases as r_{PT} is decreased from 1.0. This is because the plate with more material in the stiffener is stiffer than the one with less material in the stiffener. This trend can be observed in Fig. 5 also.

(2) Whereas, when loads are larger, inplane forces are developed and hence the deflections are reduced. These inplane forces are developed at an earlier stage of loading process for a plate with less material in stiffener. Therefore, for large loads, it can be seen that the deflection increases as r_{PT} is reduced from 1.0—a phenomenon just the reverse of what happens when the load is small. This behaviour can be clearly seen in Fig. 10 for $\theta = 45°$. For the other two values of $\theta = 0°$ and 30° also, similar trend can be observed in Figs. 8 and 9.

(3) Comparing Figs. 8–10, it can be noted that the variation in the deflection (for different values of r_{PT}) decreases as the skew angle is increased.

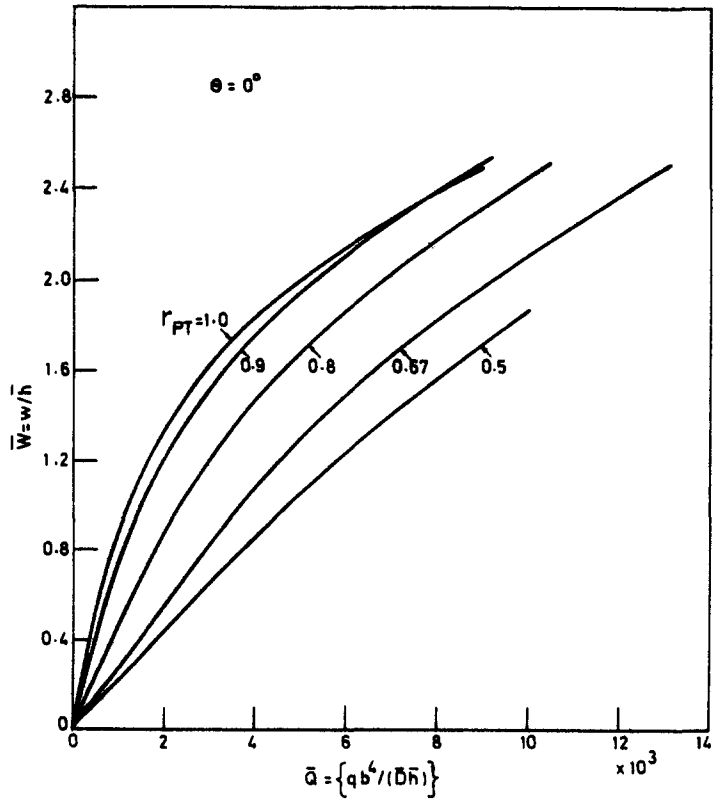

Fig. 8. Load vs deflection $\theta = 0°$.

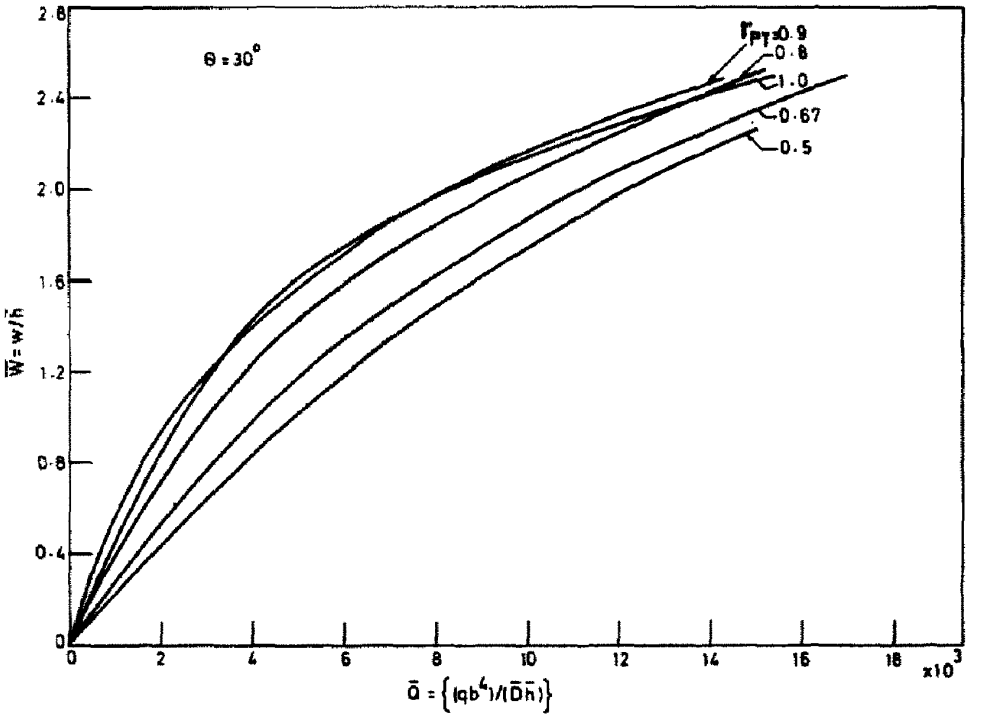

Fig. 9. Load vs deflection $\theta = 30°$

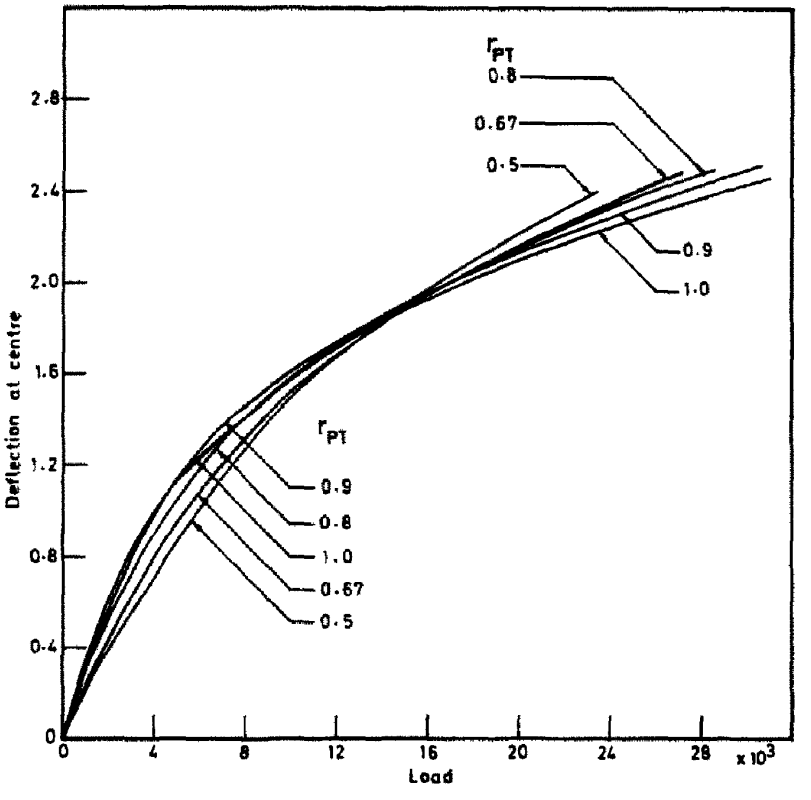

Fig. 10. Load vs deflection $\theta = 45°$.

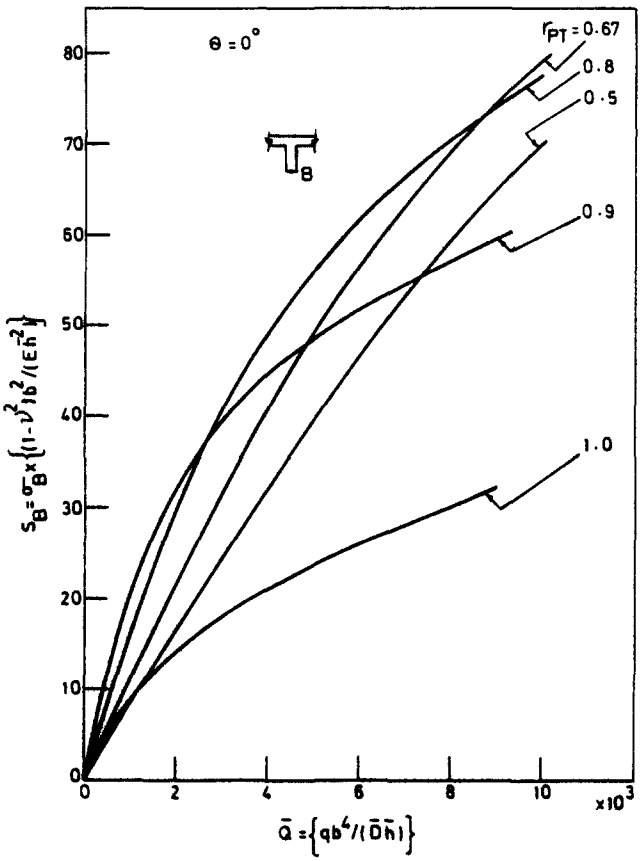

Fig. 11. Load vs stress at *B*. $\theta = 0°$

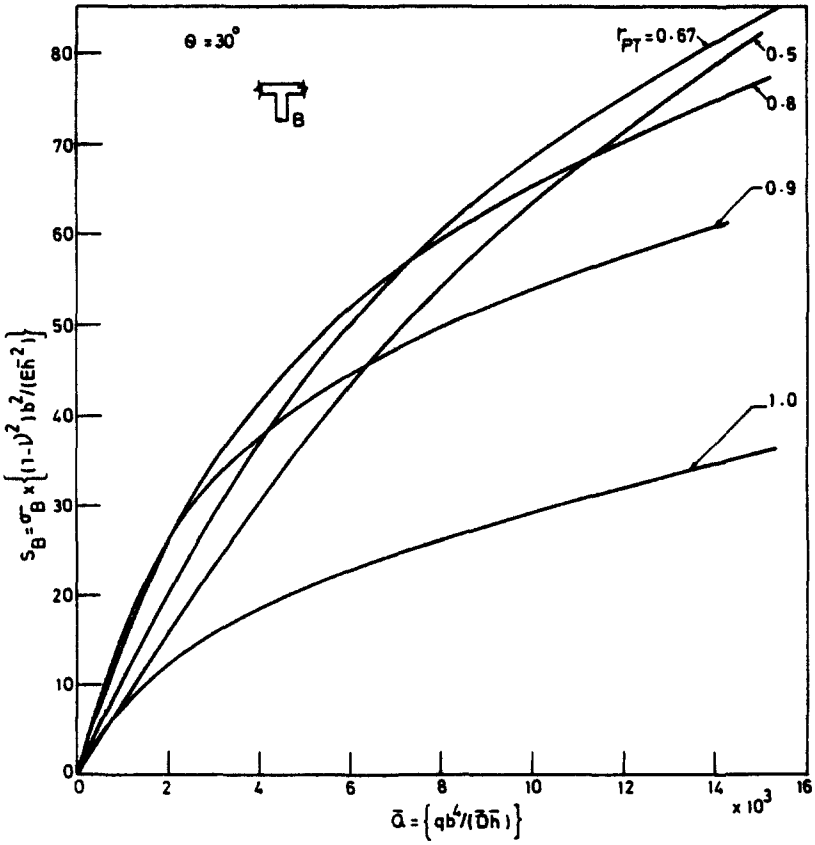

Fig. 12. Load vs stress at *B*. $\theta = 30°$.

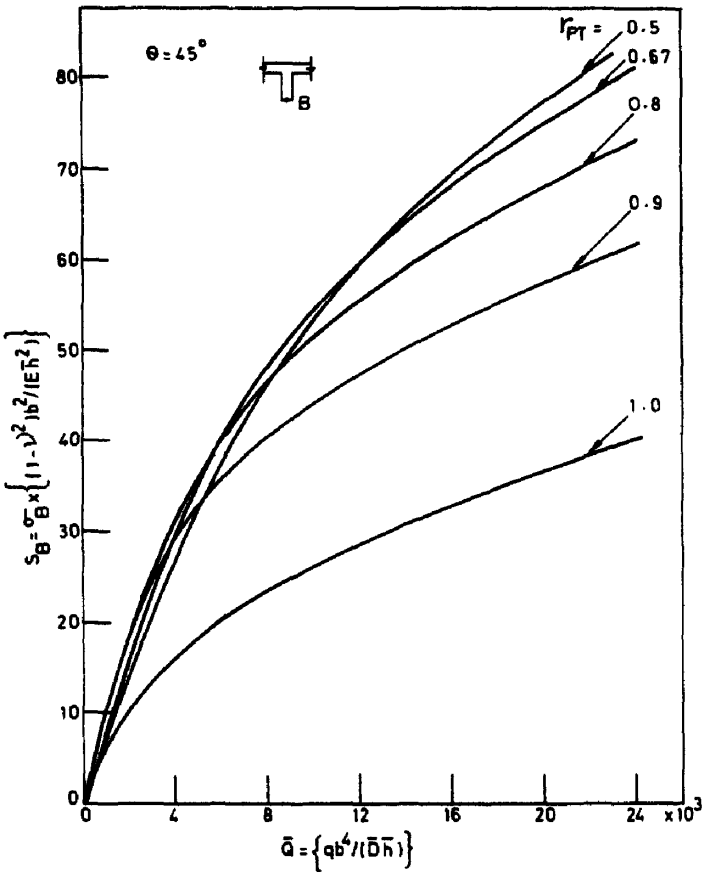

Fig. 13. Load vs stress at B. $\theta = 45°$.

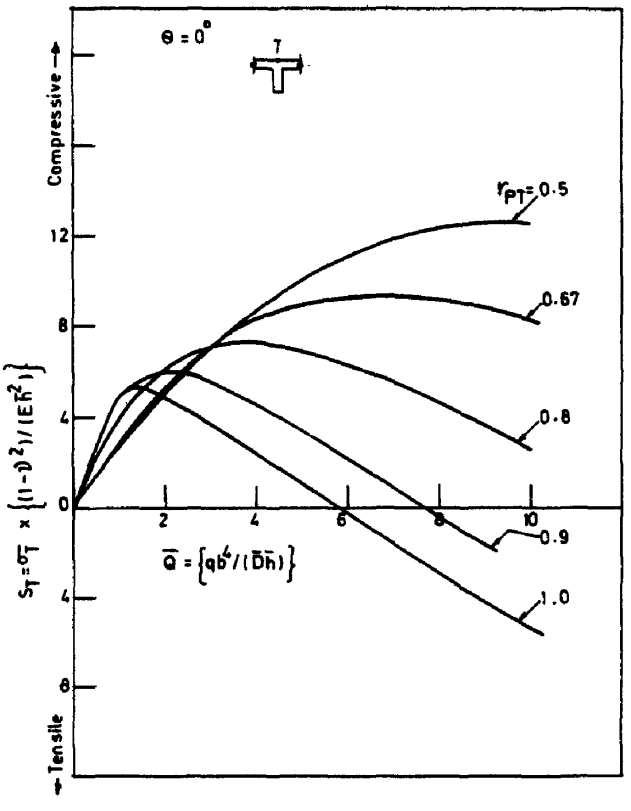

Fig. 14. Load vs stress at T. $\theta = 0°$.

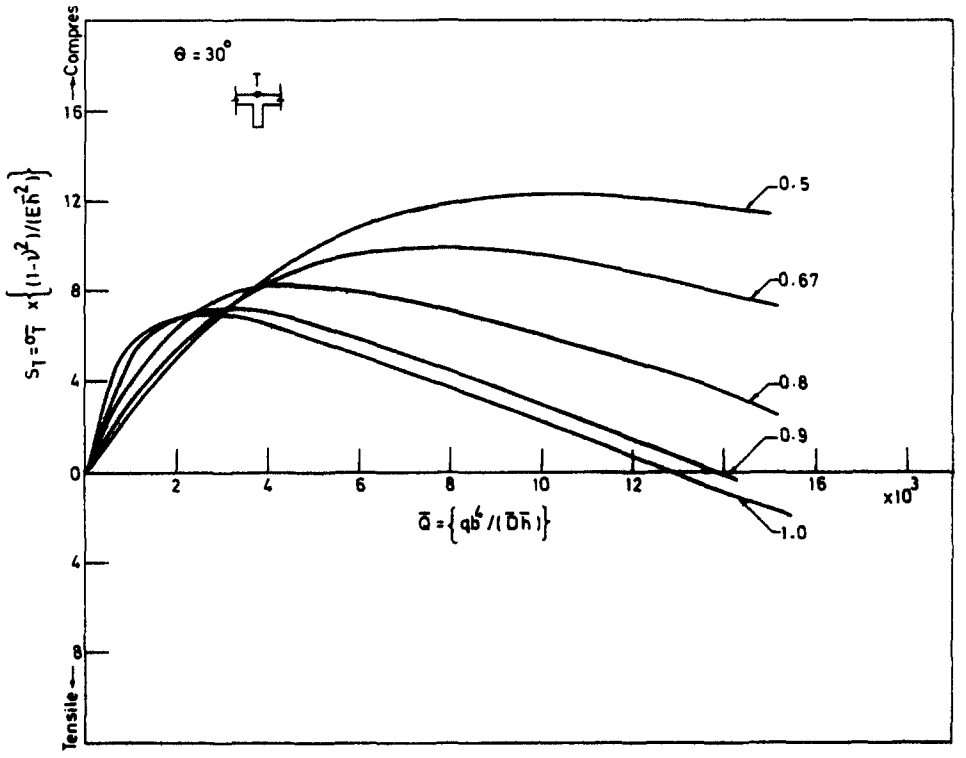

Fig. 15. Load vs stress at T. $\theta = 30°$.

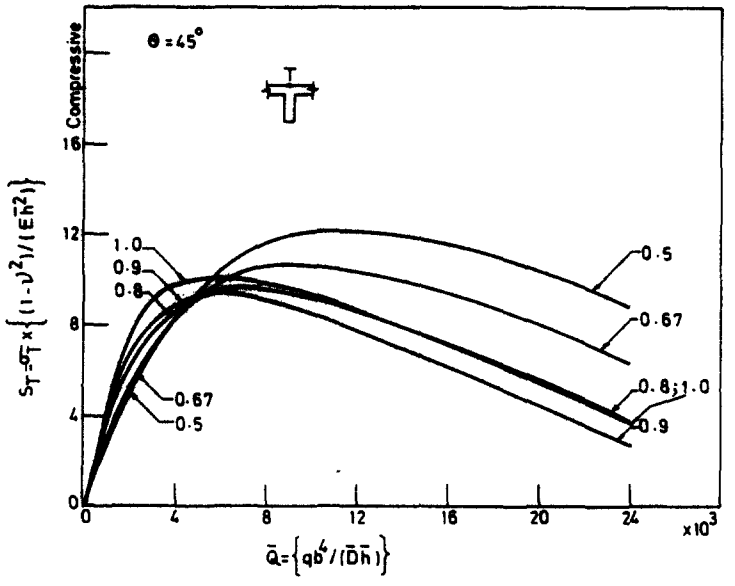

Fig. 16. Load vs stress at T. $\theta = 45°$.

(4) At B, the membrane and bending stresses are both tensile and hence they add up. Whereas at the point T (Figs. 14–16), initially for small loads, the stress is compressive. But this stress decreases due to the tensile inplane forces and for large loads, this stress becomes tensile.

CONCLUSIONS

In this paper the analysis of stiffened skew plate, a hitherto unsolved problem, has been done. The effect of the variation in the size of the stiffener and skew angle has been studied. It is believed that this will throw more light to have a better understanding of the stiffened skew plate.

REFERENCES

1. Tung Au *et al.*, Analysis of orthotropic plate bridges. *J. Struc. Div., ASCE* 133–171 (Oct. 1963).
2. Mcelman *et al.*, Static and dynamic effects of eccentric stiffening of plates and cylindrical shells, *AIAA J.* 4, 887–894 (1966).
3. W. G. Soper, Large deflection of stiffened plates. *J. App. Mech., ASME* 444–448 (Dec. 1958).
4. H. A. Hadid, Numeric analysis into the bending theory of a conoidal shell. Paper presented at the *Int. Symp. on Shell Struc. in Engg. Practice, Budapest* (1965).
5. R. S. Srinivasan and S. V. Ramachandran, Large deflection of clamped skew plates. *Computer Methods in App. Mech. and Engg.* 7, 219–233 (1976).
6. J. H. Argyris, Matrix displacement analysis of plates and shells, prolegomena to a general shell theory, Part—I, *Ingenieur-Archiv*, 35 Band 2 Heft, pp. 102–142 (1966).
7. L. S. D. Morley, *Skew Plates and Structures.* Pergamon Press, Oxford (1963).
8. K. H. Chu and P. Turula, Postbuckling behaviour of open cylindrical shells. *J. of Engg. Mech. Div., ASCE* **96**, 877–894 (1970).

APPENDIX A

Coefficients in eqns (10*a–c*)

$$a_1 = [\sec^4\theta + \{A_\alpha E_\alpha/(b_\alpha Eh)\}(1-\nu^2)]R^2$$

$$a_2 = [-2\tan\theta\sec^3\theta]R$$

$$a_3 = \sec^2\theta[\tan^2\theta + (1-\nu)/2]$$

$$a_4 = -R^2\tan\theta\sec^3\theta$$

$$a_5 = \sec^2\theta[\tan^2\theta + (1-\nu)/2 + (\nu+\tan^2\theta)]R$$

$$a_6 = -\tan\theta\sec^3\theta$$

$$a_7 = -E_\alpha S_\alpha(1-\nu^2)/(Eb_\alpha h^2)$$

$$a_{11} = -[\sec^4\theta + A_\alpha E_\alpha(1-\nu^2)/(b_\alpha Eh)]R^2$$

$$a_{21} = 2R\tan\theta\sec^3\theta$$

$$a_{31} = -\sec^2\theta[\tan^2\theta + (1-\nu)/2]$$

$$a_{12} = R\tan\theta\sec^3\theta$$

$$a_{22} = -\sec^2\theta[\nu + 2 + \tan^2\theta + (1-\nu)/2]$$

$$a_{32} = \tan\theta\sec^3\theta/R$$

$$b_1 = -R^2\tan\theta\sec^3\theta$$

$$b_2 = \sec^2\theta[\nu + 2\tan^2\theta + (1-\nu)/2]R$$

$$b_3 = -\tan\theta\sec^2\theta$$

$$b_4 = \sec^2\theta[\tan^2\theta + (1-\nu)/2]R^2$$

$$b_5 = -2R\tan\theta\sec^3\theta$$

$$b_6 = \sec^4\theta + [A_\beta E_\beta(1-\nu^2)/(b_\beta Eh)]$$

$$b_7 = -E_\beta S_\beta(1-\nu^2)/(Eb_\beta h^2 R)$$

$$b_{11} = R^2\tan\theta\sec^3\theta$$

$$b_{21} = -\sec^2\theta[\nu + 2\tan^2\theta + (1-\nu)/2]R$$

$$b_{31} = \tan\theta\sec^3\theta$$

$$b_{12} = -\sec^2\theta[\tan^2\theta + (1-\nu)/2]R$$

$$b_{22} = 2\tan\theta\sec^3\theta$$

$$b_{32} = -[\sec^4\theta + A_\beta E_\beta(1-\nu^2)/(b_\beta Eh)]/R$$

$$c_1 = [\sec^4\theta + 12(1-\nu^2)E_\alpha I_\alpha/(Eb_\alpha h^3)]R^4$$

$$c_2 = -4R^3\tan\theta\sec^3\theta$$

$$c_3 = 2\sec^2\theta[1 + 3\tan^2\theta]R^2$$

$$c_4 = -4R\tan\theta\sec^3\theta$$

$$c_5 = \sec^4\theta + [12(1-\nu^2)E_\beta I_\beta/(Eb_\beta h^3)]$$

$$c_6 = -[12(1-\nu^2)E_\alpha S_\alpha/(Eb_\alpha h^2)]R^4$$

$$c_7 = -[12(1-\nu^2)E_\beta S_\beta/(Eb_\beta h^2)]R$$

$$c_{11} = 12[\sec^4\theta + (1-\nu^2)A_\alpha E_\alpha/(b_\alpha hE)]R^4$$

$$c_{12} = -12R^3\tan\theta\sec^3\theta$$

$$c_{13} = -12R^4\tan\theta\sec^3\theta$$

$$c_{14} = 12R^3\sec^2\theta(\nu + \tan^2\theta)$$

$$c_{15} = 6[\sec^4\theta + A_\alpha E_\alpha(1-\nu^2)/(b_\alpha Eh)]R^4$$

$$c_{16} = -12R^3\tan\theta\sec^3\theta$$

$$c_{17} = 6R^2\sec^2\theta(\nu + \tan^2\theta)$$

$$c_{21} = -24R^3\tan\theta\sec^3\theta$$

$$c_{22} = 24R^2\sec^2\theta[\tan^2\theta + (1-\nu)/2]$$

$$c_{23} = 24R^3\sec^2\theta[\tan^2\theta + (1-\nu)/2]$$

$$c_{24} = -24R^2\tan\theta\sec^3\theta$$

$$c_{25} = -12R^3\tan\theta\sec^3\theta$$

$$c_{26} = 24R^2\sec^2\theta[\tan^2\theta + (1-\nu)/2]$$

$$c_{27} = -12R\tan\theta\sec^3\theta$$

$$c_{31} = 12R^2\sec^2\theta(\nu + \tan^2\theta)$$

$$c_{32} = -12R\tan\theta\sec^2\theta$$

$$c_{33} = -12R^2\tan\theta\sec^2\theta$$

$$c_{34} = 12R[\sec^4\theta + (1-\nu^2)A_\beta E_\beta/(b_\beta hE)]$$

$$c_{35} = 6R^2\sec^2\theta(\nu + \tan^2\theta)$$

$$c_{36} = -12R\tan\theta\sec^3\theta$$

$$c_{37} = 6[\sec^4\theta + (1-\nu^2)A_\beta E_\beta/(b_\beta Eh)]$$

$$c_8 = 12(1-\nu^2)E_\alpha S_\alpha/(b_\alpha Eh^2)$$

and

$$c_9 = 12(1-\nu^2)E_\beta S_\beta/(b_\beta Eh^2).$$